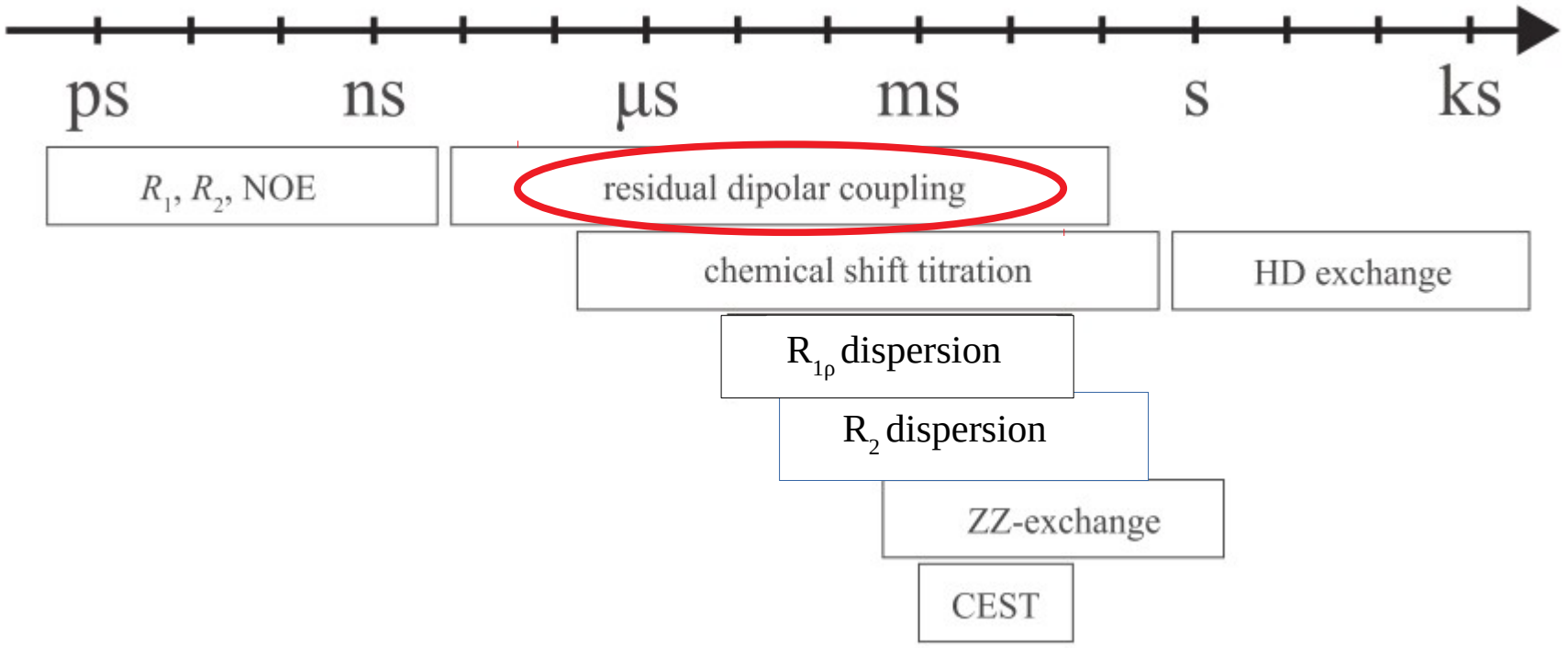
ps
ns
μs
ms
s
ks
R_1, R_2, NOE
residual dipolar coupling
chemical shift titration
HD exchange
$R_{1\rho}$ dispersion
R_2 dispersion
ZZ-exchange
CEST

Dipolar couplings

Atom Pair A - B	Dipolar Interaction Value D^{AB}_{max}
HN - N	-21,585 Hz
HN - C'	6,666 Hz
C' - N	-2,609 Hz
HA - CA	44,539 Hz
C' - CA	4,285 Hz
CA - CB	4,150 Hz

Motion averages these values to near zero. However in proteins and nucleic acids, the magnetic susceptibility anisotropy, due to aromatic rings and carbonyls, is not completely averaged to zero and (small) residual dipolar couplings (RDC) can be measured.

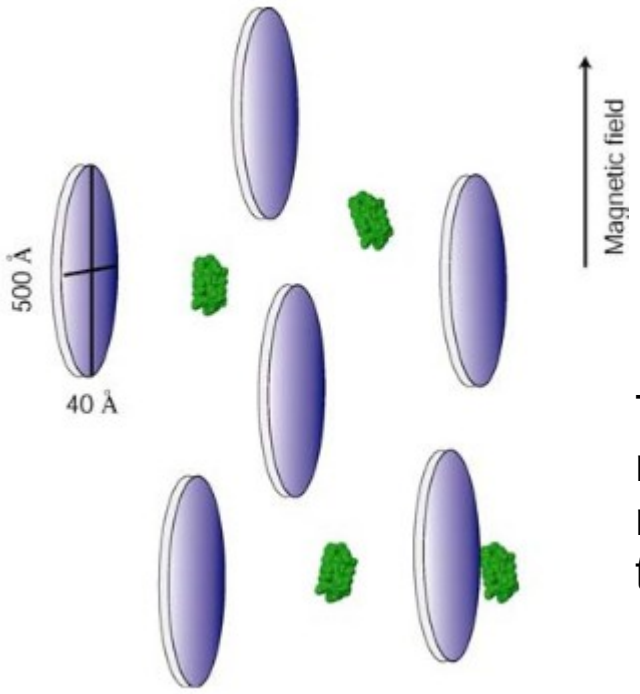

The most common way to measure RDCs is to dissolve the molecule under study in an alignment media that has other molecules or structures that align in the magnetic field due to their large magnetic susceptibility anisotropy

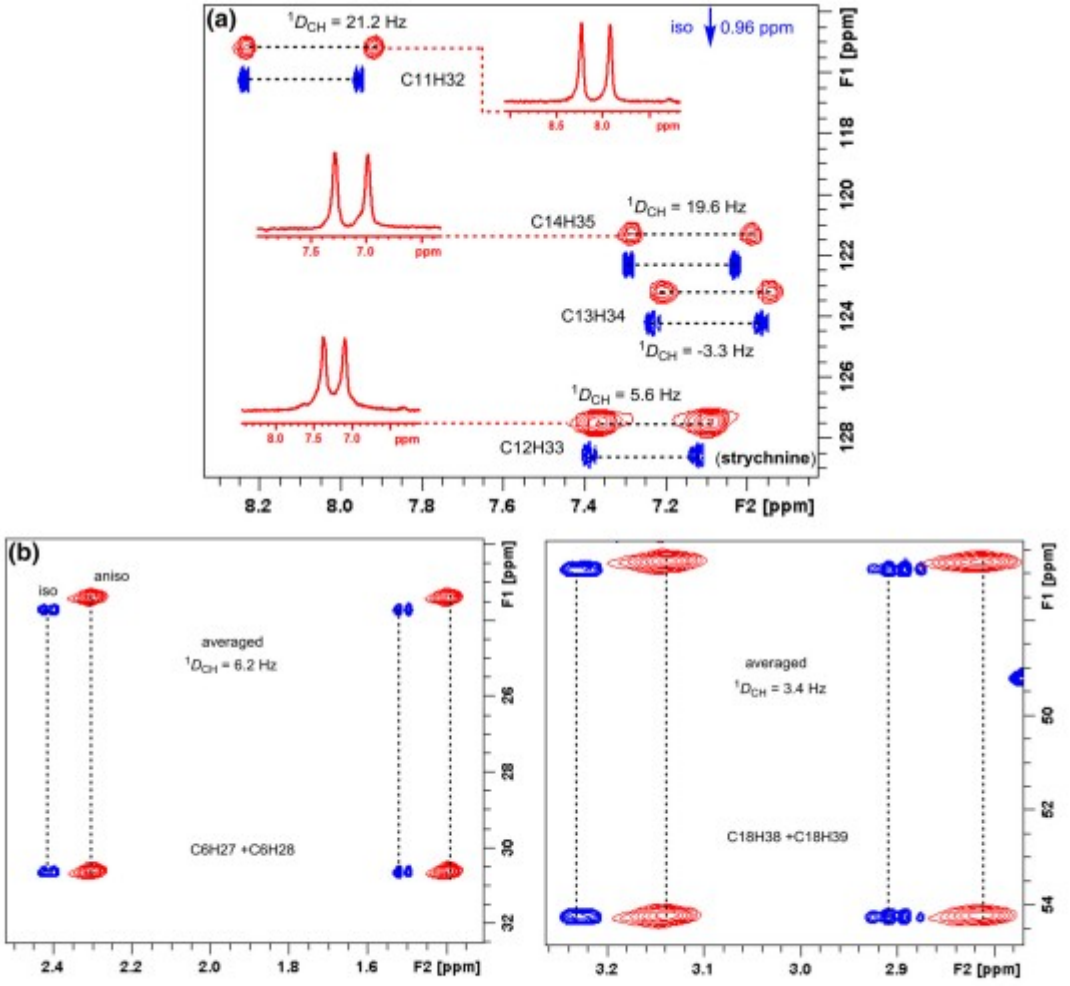

Fig. 5 (**a**) Expanded CLIP-HSQC spectra of strychnine in the isotropic $CDCl_3$ phase (blue contours) and in anisotropic 1,1-PIAF-OBn LCs (red contours). The inserted trace from the anisotropic 2D spectra (C11/H32, C12/H33, C13/H34 and C14/H35) illustrates the favorable line widths. (**b**) Expanded regions of methylene C6/H27 and C6/H28, C18/H38 and C18/H39 signals in the JSB-HSQC experiment for measuring the $^1D_{CH}$ couplings

Li, GW., Liu, H., Qiu, F. et al. Residual Dipolar Couplings in Structure Determination of Natural Products. Nat. Prod. Bioprospect. 8, 279–295 (2018). https://doi.org/10.1007/s13659-018-0174-x

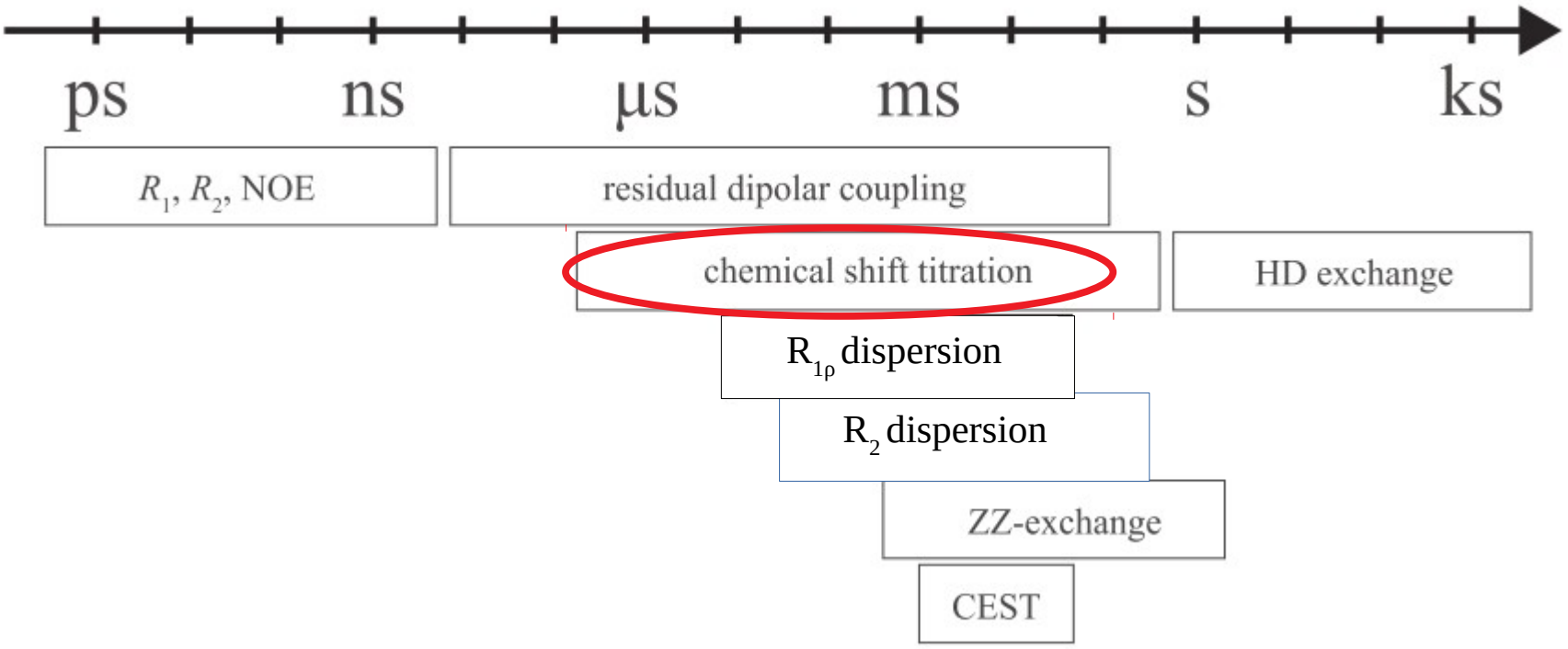
ps
ns
µs
ms
s
ks
R_1, R_2, NOE
residual dipolar coupling
chemical shift titration
HD exchange
$R_{1\rho}$ dispersion
R_2 dispersion
ZZ-exchange
CEST

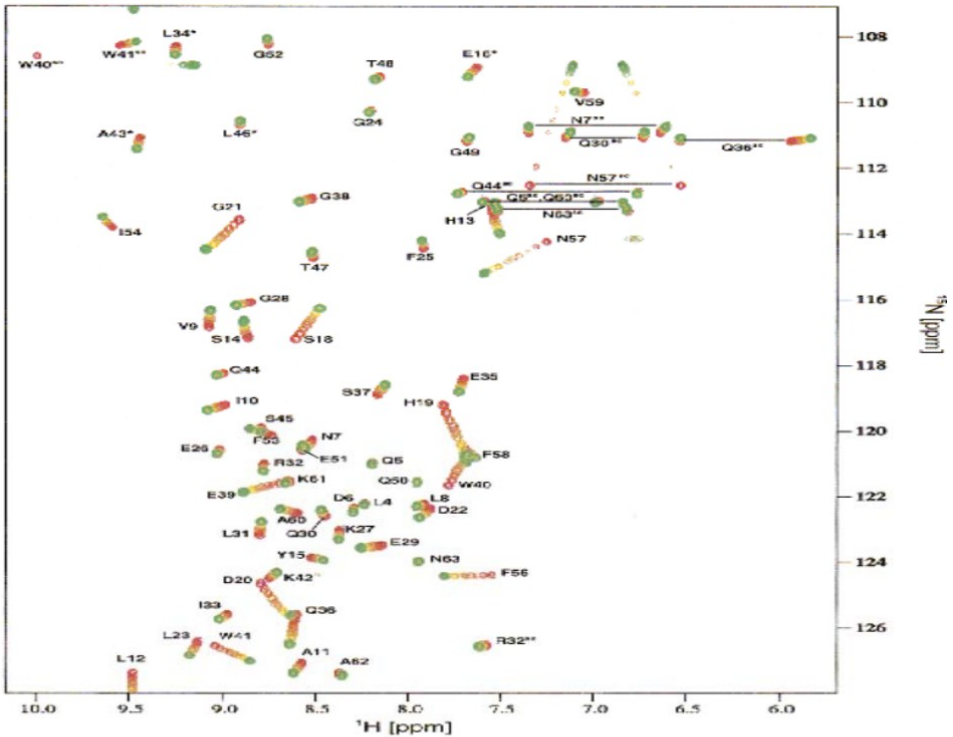

NMR titration experiment showing the changes in the ^{1}H-^{15}N HSQC spectrum of free LckSH3 (red) upon gradual addition of Tip(173-185). Resonances belonging to the spectra after the final step of the titration (4-fold molar excess of Tip) are shown in green.

Structural Investigation of the Binding of a Herpesviral Protein to the SH3 Domain of Tyrosine Kinase Lck, Kristian Schweimer, Silke Hoffmann, Finn Bauer, Ute Friedrich, Christian Kardinal, Stephan M. Feller, Brigitte Biesinger, and Heinrich Sticht Biochemistry 2002 41 (16), 5120-5130 DOI: 10.1021/bi015986j

Nonlinear plots do not necessarily imply multiple interactions: they can also be caused by something more complicated than a two-state binding interaction. A conformational change, either as will also give rise to curved titrations (and very often broadened signals), and can produce some remarkably messy and intractable results.

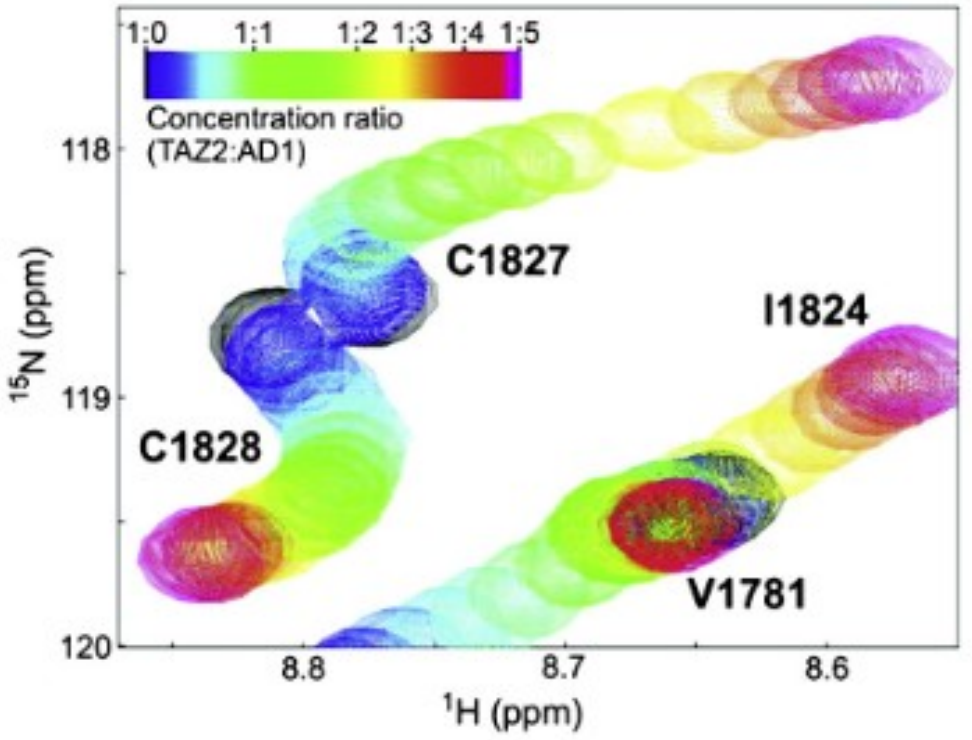

Fig. 11. A small region of the ^{15}N HSQC spectrum of ^{15}N-labelled TAZ2 titrated with unlabelled p53 AD1 domain (residues 13–37). The colour of the cross-peaks changes from black (free protein) to magenta (1:5 ratio). Adapted with permission from M. Arai et al. J. Am. Chem. Soc. 2012 **134**:3792–3803. Copyright (2012) American Chemical Society.

Mike P. Williamson, Using chemical shift perturbation to characterise ligand binding, Progress in Nuclear Magnetic Resonance Spectroscopy, Volume 73, 2013, Pages 1-16, ISSN 0079-6565, https://doi.org/10.1016/j.pnmrs.2013.02.001.

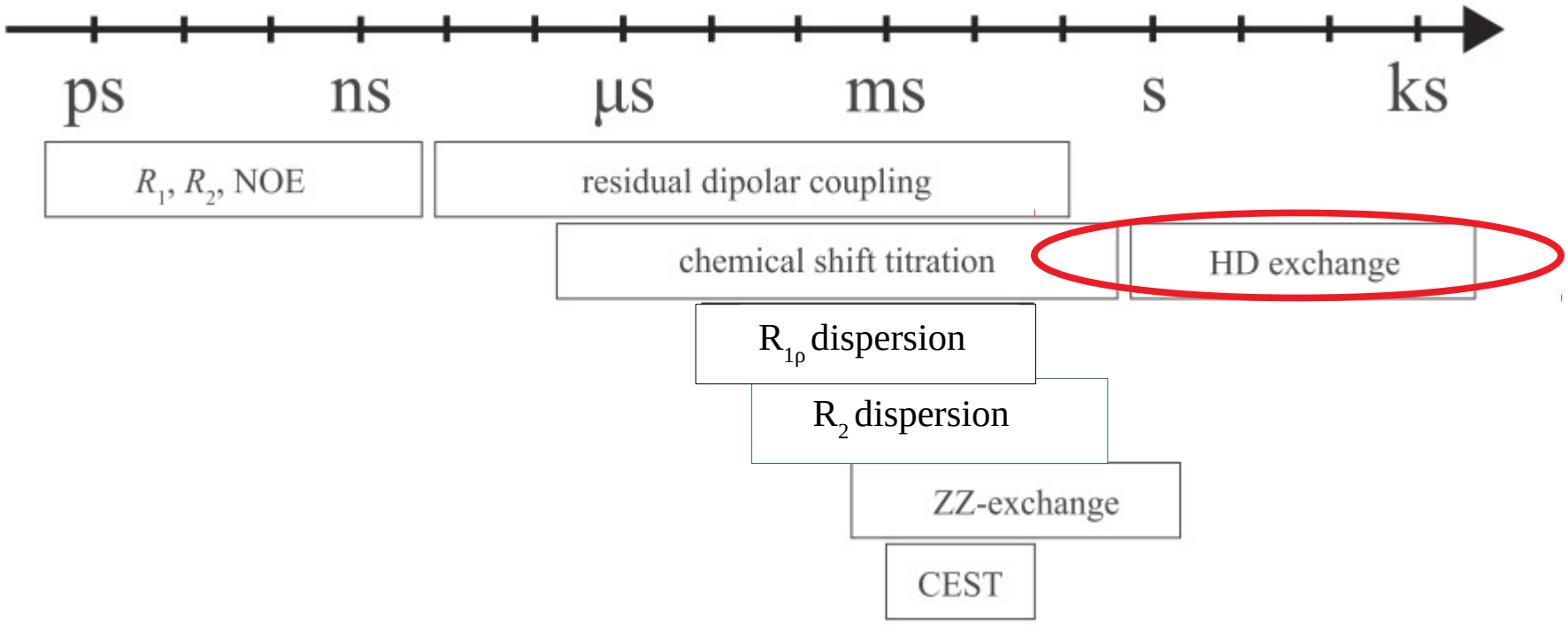
ps
ns
μs
ms
s
ks
R_1, R_2, NOE
residual dipolar coupling
chemical shift titration
HD exchange
$R_{1\rho}$ dispersion
R_2 dispersion
ZZ-exchange
CEST

Hydrogen exchange

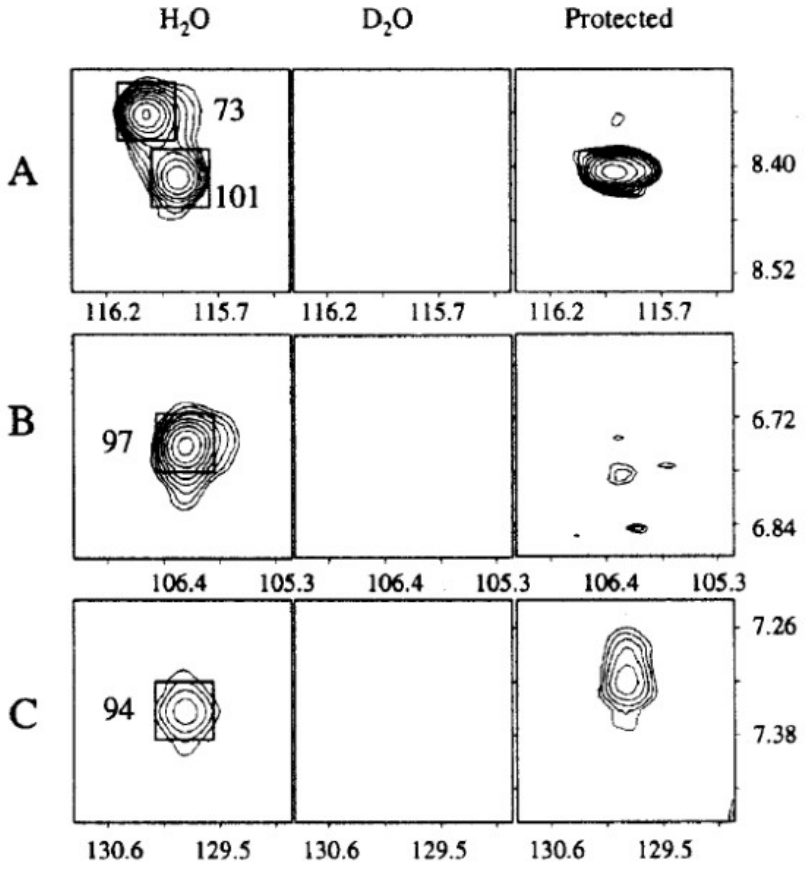

FIG. 2. **Representative exchange data for mAb 7A1.** Portions of the HSQC spectra of Der p 2 containing resonances from residues 73, 101 (*panel A*), 97 (*panel B*), and 94 (*panel C*) are shown. The *left column* of spectra were obtained for a sample in H_2O. The *middle column* of spectra were obtained from a sample of Der p 2 in D_2O. The *right column* (*Protected*) of spectra were obtained from a sample that was bound to mAb 7A1 for 48 h in the presence of D_2O.

Mueller, Geoffrey & Smith, Alisa & Chapman, Martin & Rule, Gordon & Benjamin, David. (2001). Hydrogen Exchange Nuclear Magnetic Resonance Spectroscopy Mapping of Antibody Epitopes on the House Dust Mite Allergen Der p 2. The Journal of biological chemistry. 276. 9359-65. 10.1074/jbc.M010812200.

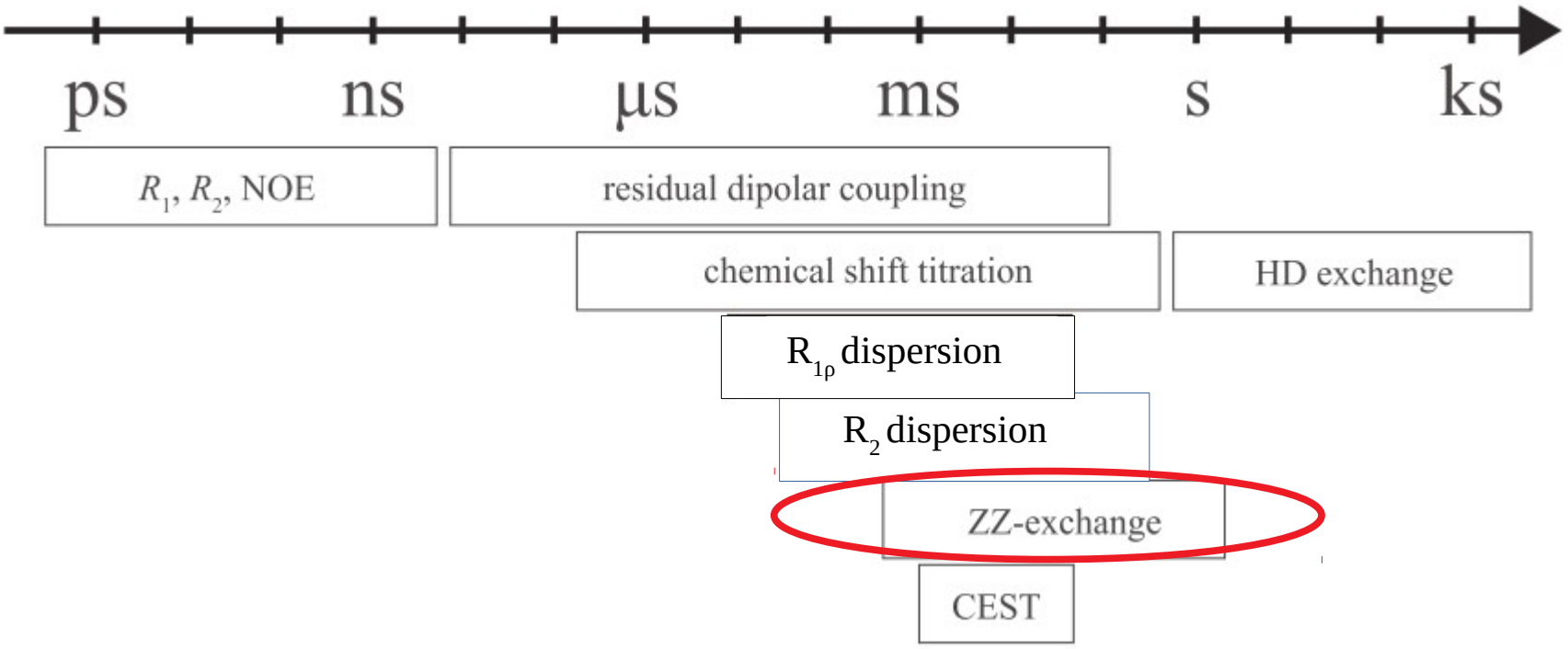
ps
ns
μs
ms
s
ks
R_1, R_2, NOE
residual dipolar coupling
chemical shift titration
HD exchange
$R_{1\rho}$ dispersion
R_2 dispersion
ZZ-exchange
CEST

ZZ-exchange to measure conformational changes

$$H_Z N_Z \rightleftarrows H'_Z N'_Z$$

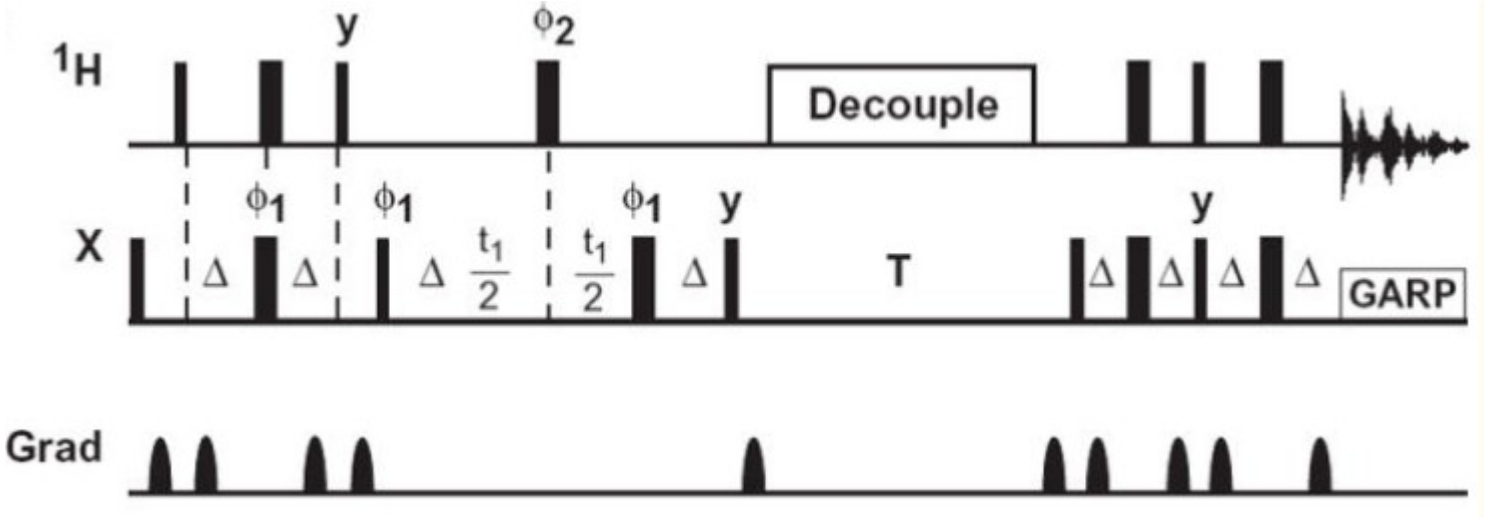

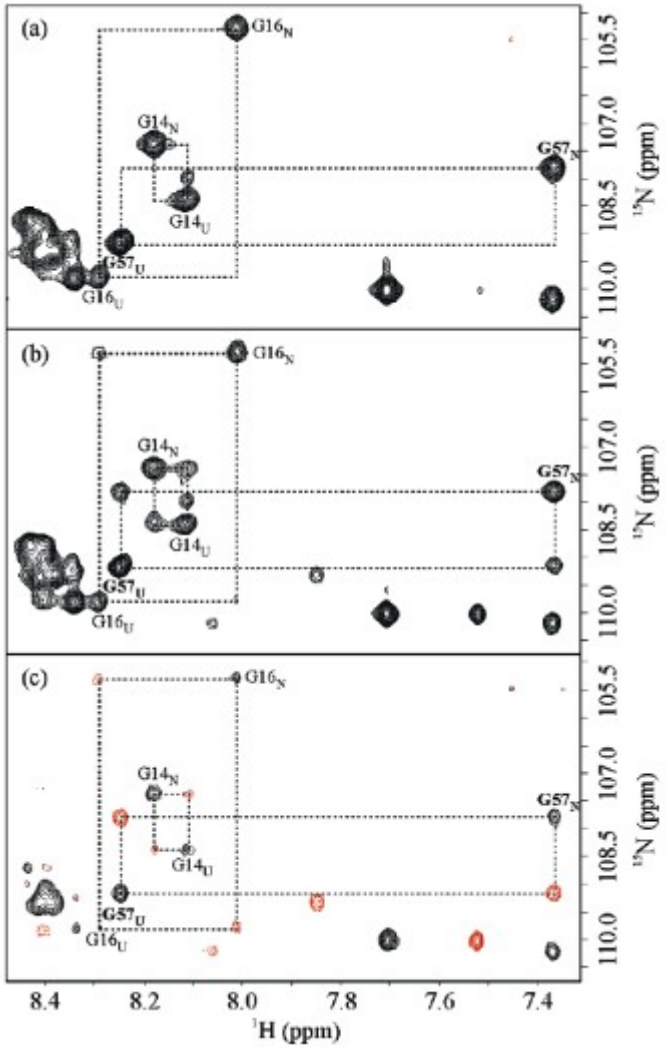

Figure 3. Section of 2D ^{15}N ZZ exchange spectra of CspB at 750 MHz in 20 mM Na-cacodylate/HCl pH 7.0 at 25 °C in the presence of 3.1 M urea and an exchange delay of 60 ms. (a) The reference spectrum contains solely cross-peaks of the native and the unfolded state (auto cross-peaks). (b) The ZZ exchange spectrum shows auto cross-peaks with reduced intensity as well as additional exchange cross-peaks. (c) The difference spectrum of the reference and the exchange spectrum (a−b) yields residual positive intensities for the auto cross-peaks (solid black line) and negative intensities for the exchange cross-peaks (solid red line). The assignment of cross-peaks is given in the spectra. Dashed lines connect auto and exchange cross-peaks of one backbone amide.

NMR Spectroscopic Characterization of Millisecond Protein Folding by Transverse Relaxation Dispersion Measurements Markus Zeeb and Jochen Balbach Journal of the American Chemical Society 2005 127 (38), 13207-13212 DOI: 10.1021/ja051141+

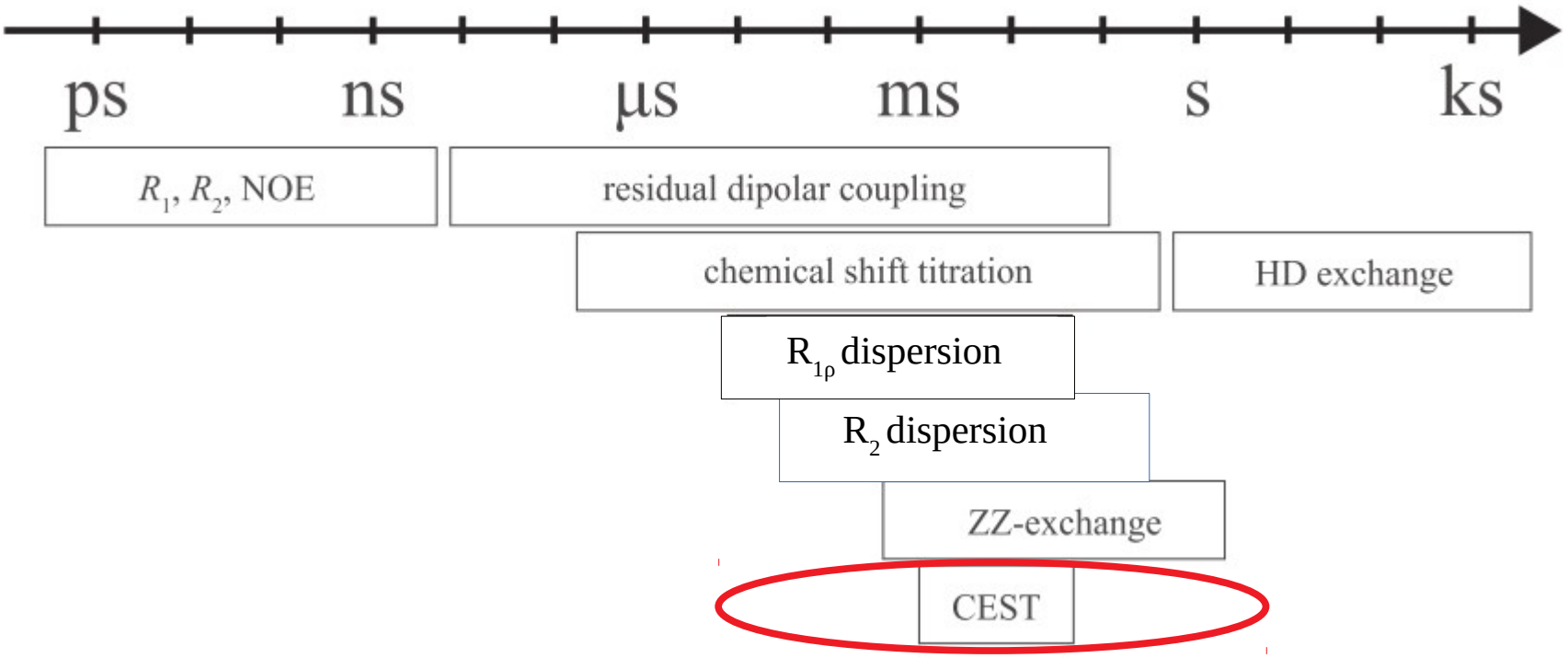
ps
ns
μs
ms
s
ks
R_1, R_2, NOE
residual dipolar coupling
chemical shift titration
HD exchange
$R_{1\rho}$ dispersion
R_2 dispersion
ZZ-exchange
CEST

CEST- Chemical exchange saturation transfer (Anderson 1956)
DEST- Dark state exchange saturation transfer

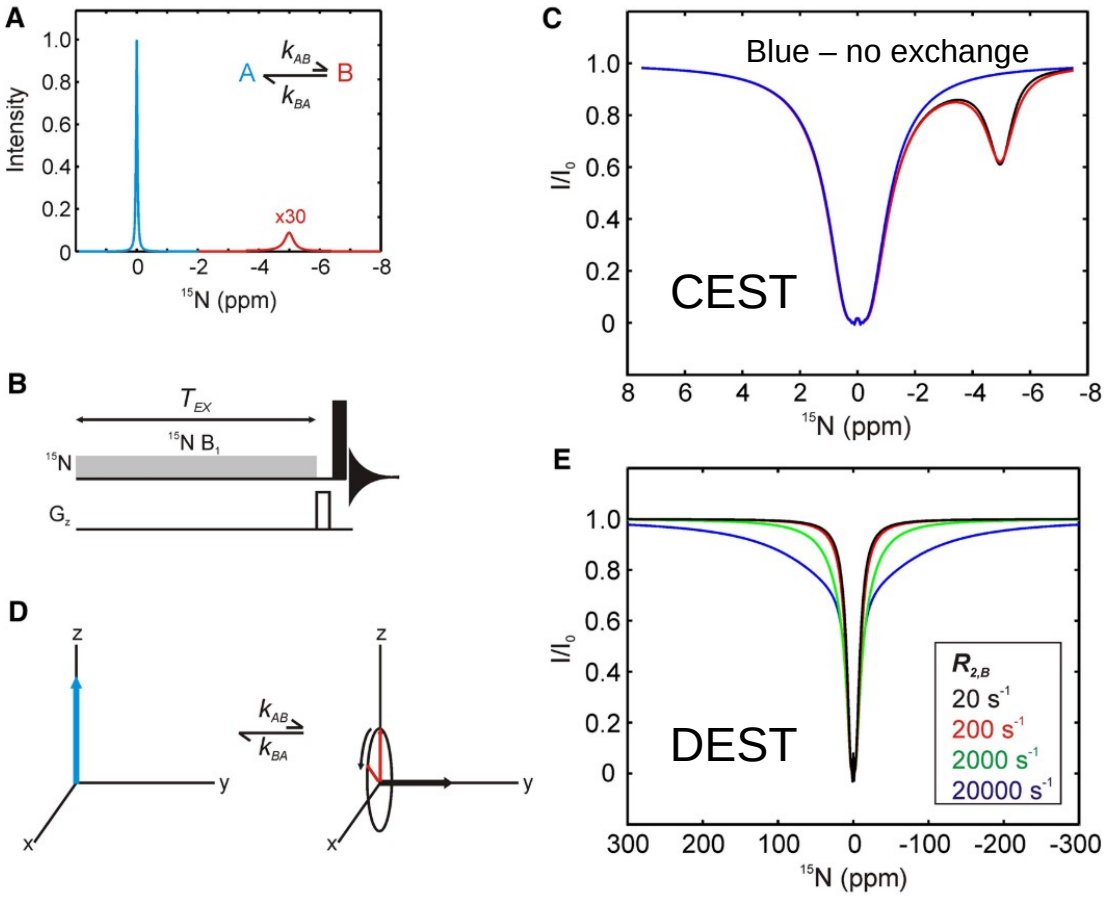

The distinction between CEST and DEST is that while CEST exploits differences in chemical shifts between exchanging states, DEST distinguishes between states on the basis of their very different linewidths that would arise in a system in which a biomolecule exchanges between a free state and one that is bound to a very large complex

Nicholas J. Anthis and G. Marius Clore, Quarterly Reviews of Biophysics48, 1 (2015), pp. 35–116

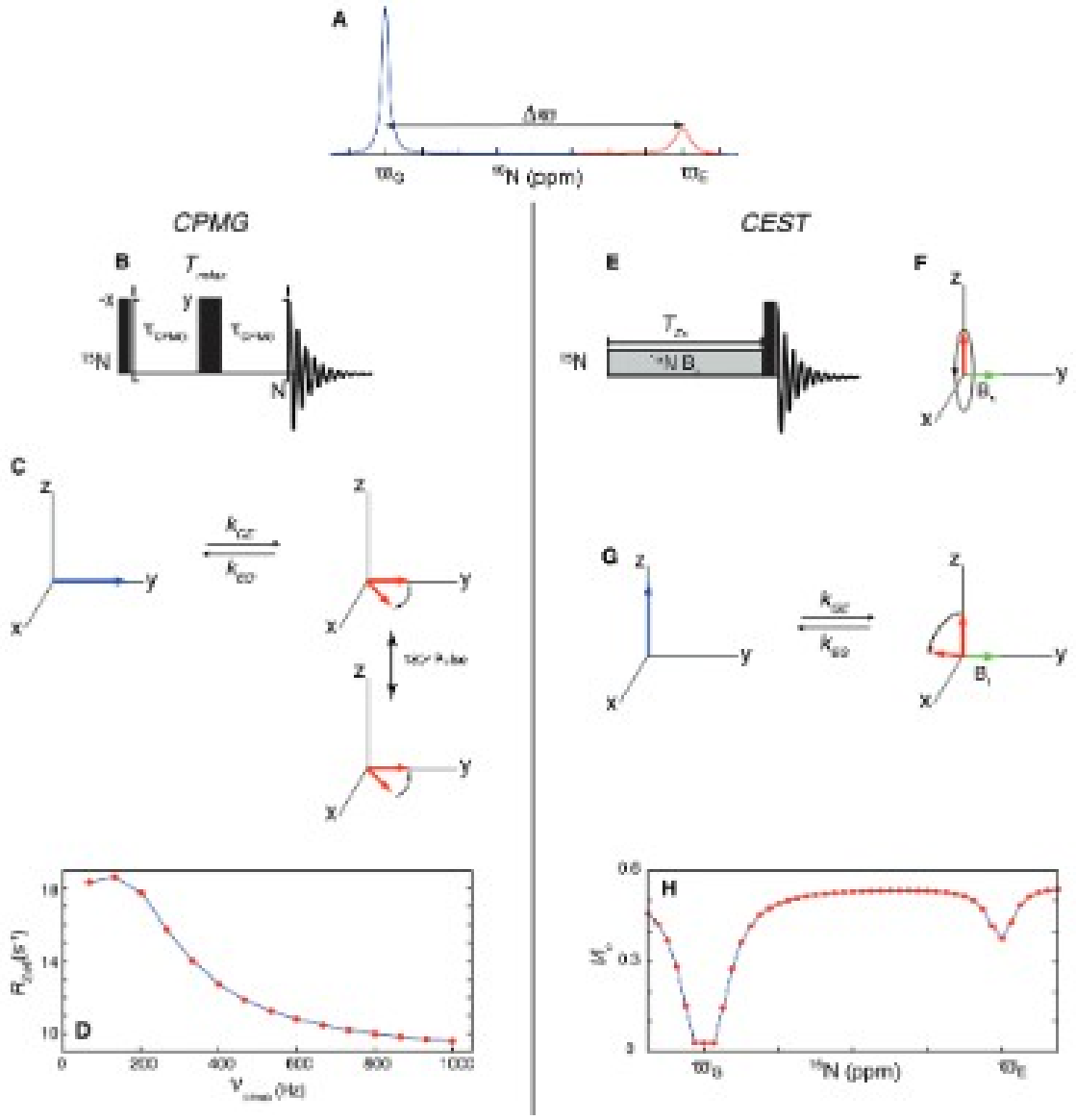

Figure 1.Comparison of the standard CPMG experiment with the weakB1CEST experiment proposed here. (A)15N spectrum of an isolated spinexchanging between two states with chemical shiftsωGandωE. The minor state is shown in the spectrum for purposes of illustration but cannot beobserved in the systems of interest. (B) Basic CPMG experiment, with narrow and wide pulses denoting 90°and 180°flip angles, respectively.A variable number (N) of 180°refocusing pulses is applied during a constant-time relaxation element of durationTrelax. (C) Illustration of themechanism underlying the CPMG experiment, with the major-state peak (blue) assumed to be on resonance. The 180°pulses invert the sense inwhich“excited-state”spins (red magnetization) precess around the external magneticfield (B0). Stochastic modulation of the chemical shifts of theinterconverting spins leads to a dephasing of the magnetization. (D) Typical relaxation dispersion curve obtained by quantifying the peak intensitiesin a CPMG experiment. (E) Schematic of the CEST experiment. A weakB1field is applied along theyaxis (green) for a timeTEXbefore acquisitionof the spectrum. (F) When theB1field is on resonance with the minor state, precession occurs around theyaxis, in analogy to what is shown in (C)for the CPMG experiment. (G) Precession leads to a phase accumulation with respect to the magnetization in the major state and a subsequentreduction in the magnetization intensity of the major state from the constant exchange between states. (H) Intensity profile obtained by quantifyingthe intensity of the visible-state peak as a function of position of the weakB1irradiationfield. The ratioI/I0is plotted, whereIis the intensity after anirradiation period of durationTEXandI0is the intensity whenTEX= 0. There is a loss of intensity when the weak continuous-wavefield is resonantwith the major and minor states

Studying “Invisible” Excited Protein States in Slow Exchange with a Major State Conformation Pramodh Vallurupalli, Guillaume Bouvignies, and Lewis E. Kay Journal of the American Chemical Society 2012 134 (19), 8148-8161 DOI: 10.1021/ja3001419

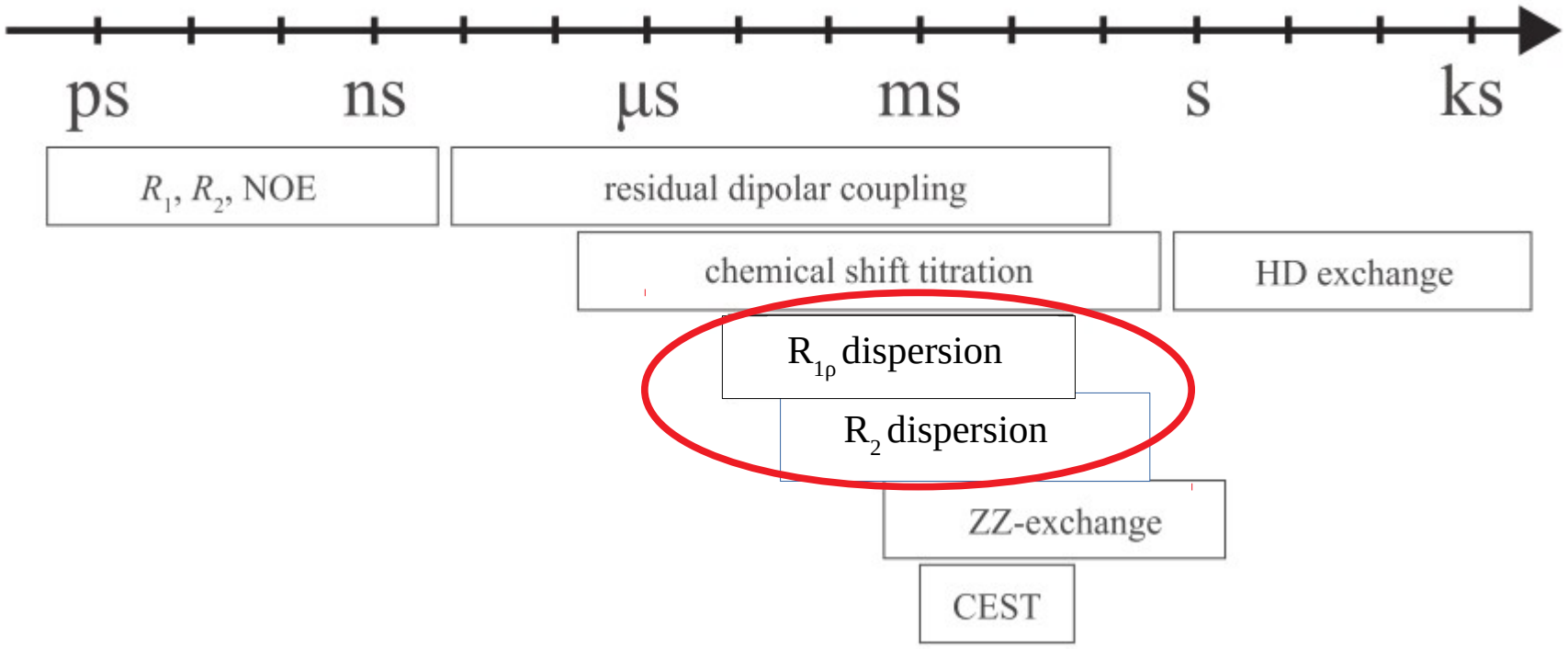
ps
ns
μs
ms
s
ks
R_1, R_2, NOE
residual dipolar coupling
chemical shift titration
HD exchange
$R_{1\rho}$ dispersion
R_2 dispersion
ZZ-exchange
CEST

NMR Dynamics and Exchange

Equal Population of Exchange Sites

No exchange:

$$W_{1/2} = \frac{1}{\pi T_2}$$

With exchange:

$$W_{1/2} = \frac{1}{\pi T_2} + \frac{1}{\pi \tau_{ex}}$$

$$k = \frac{1}{\tau_{ex}}$$

slow

Increasing Exchange Rate

fast

k = 0.1 s^{-1}

k = 5 s^{-1}

k = 10 s^{-1}

k = 20 s^{-1}

k = 40 s^{-1}

coalescence
k = 88.8 s^{-1}

k = 200 s^{-1}

k = 400 s^{-1}

k = 800 s^{-1}

k = 10,000 s^{-1}

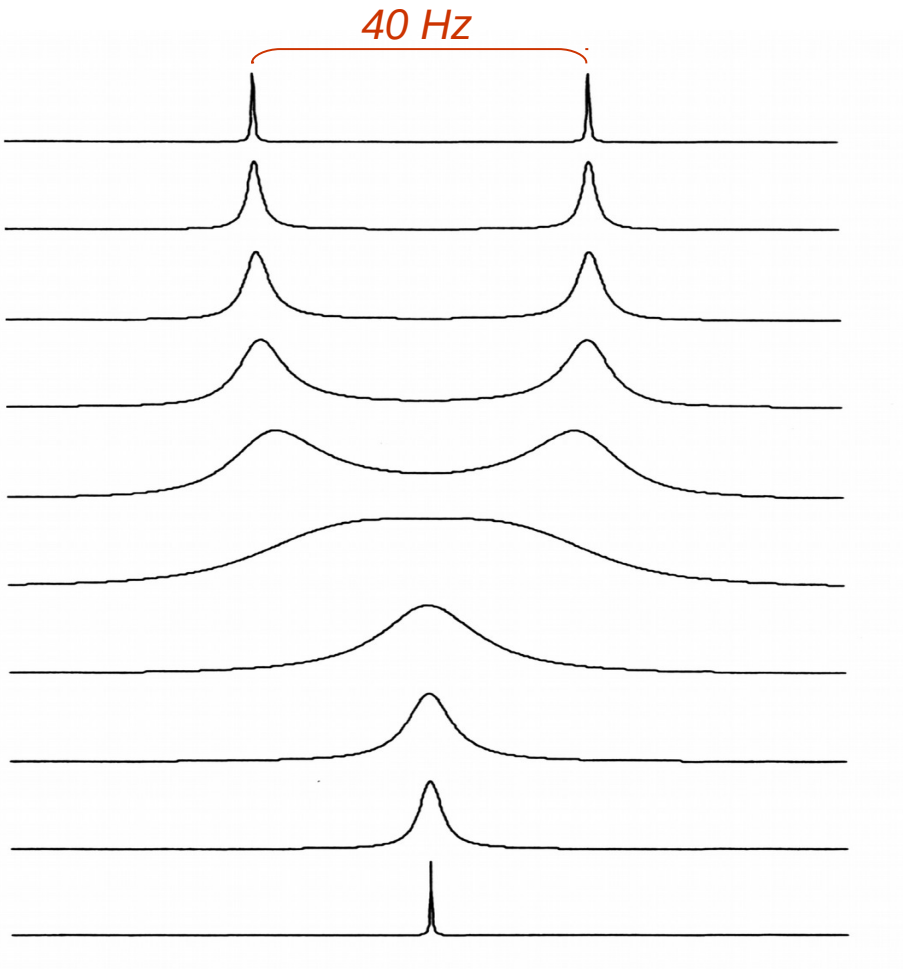

NMR Dynamics and Exchange

Unequal Population of Exchange Sites

- differential broadening below coalescence
  - ***lower populated peak broadens more***

Exchange rate depends on population (p):

$$k_A = k_B \frac{p_B}{p_A}$$

Above coalescence:

$$\nu_{avg} = \frac{\nu_A p_A + \nu_B p_B}{p_A + p_B}$$

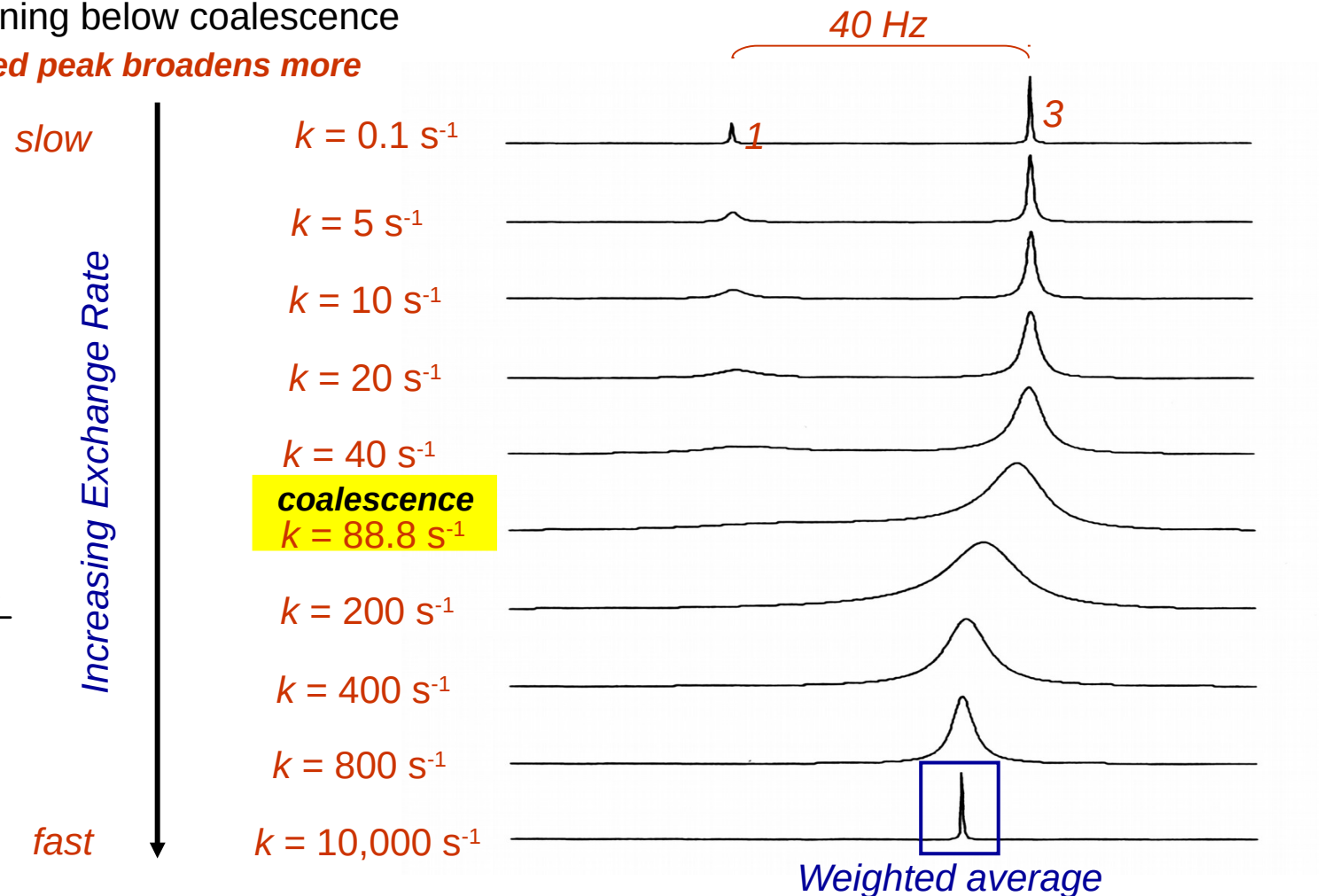

Erwin Hahn
Nov 1953

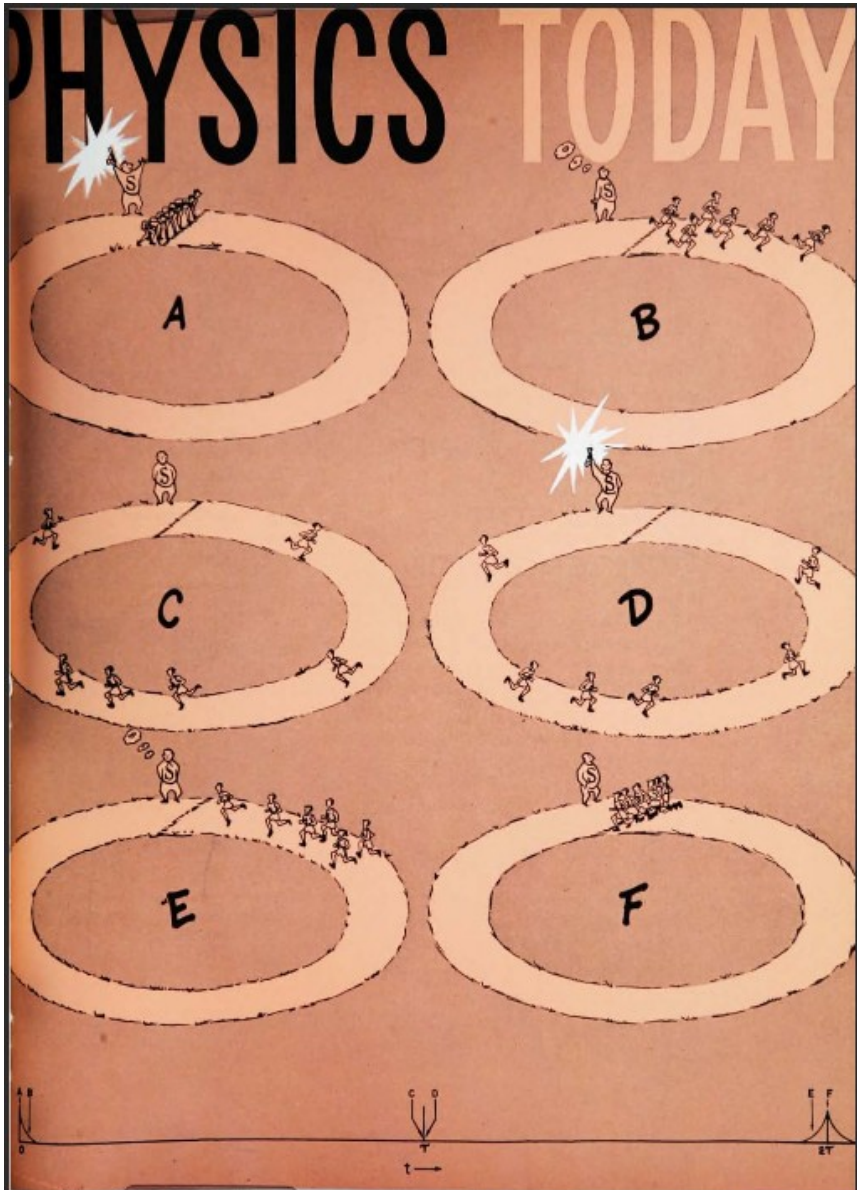

FREE NUCLEAR INDUCTION

By E. L. Hahn

Unusually clear measurements of the time precession of nuclear magnetic moments and other properties of nuclei have become possible with the development of the free induction "spin echo" technique in the still new science of nuclear magnetic resonance.

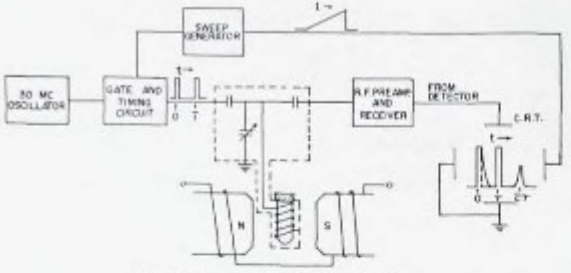

Fig. 1. Arrangement for obtaining spin echoes.

THE STUDY of nuclear magnetic resonance or nuclear induction, a recent field of research for which F. Bloch [1] and E. M. Purcell [2] have been awarded the Nobel Prize, has been carried out by a variety of techniques. The usual approach has been to observe the nuclear resonance of an ensemble of nuclear moments in a large static magnetic field as a function of a slow change in this field. Meanwhile, a small radio-frequency field is applied continuously to the nuclear sample in a direction perpendicular to the large field. An alternative method to this steady state or "slow passage" technique is one by which the radio-frequency energy is applied to the sample in the form of short, intense pulses, and nuclear signals are observed after the pulses are removed. The effects which result can be compared to the free vibration or "ringing" of a bell, a term often applied to the free harmonic oscillations of a shocked inductive-capacitive (LC) circuit. The circuit is first supplied with electrical energy from some source, and the supply of energy is suddenly removed. The LC circuit then remains for a time in the "excited state", and the energy is gradually dissipated into heat, mostly in the circuit resistance. Similarly the atom or nucleus in the excited state can store energy for a time before it is completely dissipated, and in the case discussed here, the free oscillation or precession of an ensemble of nuclear spins in a large static field provides the ringing process.

It appears that the topic of free nuclear precession or "spin echoes", as it will be called here, can be classified under one of the following two approaches to the study of excited states: (a) A study can be made of the absorption or emission of radiation by a system. The system gains or loses radiation (or particles), and the experiment involves a measurement of the energy and intensity of radiation. (b) The behavior of some systems can be studied, not by observing directly whether they gain or lose radiation, but by detecting their mode of motion under the influence of applied *static* electric and magnetic fields. While observing such motion it is possible to infer whether or not the system has gained or lost radiation in the past.

It is well known that the latter approach is involved in the Rabi molecular beam technique [3] in which molecules and atoms are deflected in space. Also, this approach applies to the free nuclear precession or induction effect. The viewpoint of the experiment has been particularly emphasized by Bloch,[1] and is very much like the scheme for detecting the ringing of a tuned LC circuit. A pickup loop can be coupled to the magnetic flux about the inductance and a voltage of induction is measured. In the actual experiment the magnetic induction is provided by the precession of an ensemble of nuclear moments in a static magnetic field after the moments are "shocked" into a coherent state of precession by one or more pulses of radio-frequency magnetic field. One might classify this measurement under (a) above, and deduce that here the ringing of the system is measured by detecting the stored magnetic energy which the system dissipates. Certainly some radio-frequency (rf) energy is consumed by the loop which couples to the ringing LC circuit, but this can be made

E. L. Hahn, a physicist at the Watson Laboratory and a member of the physics staff at Columbia University, received his PhD at the University of Illinois in 1949. He was a National Research Council Fellow and instructor at Stanford University in 1951–52.

Spin echo with exchange

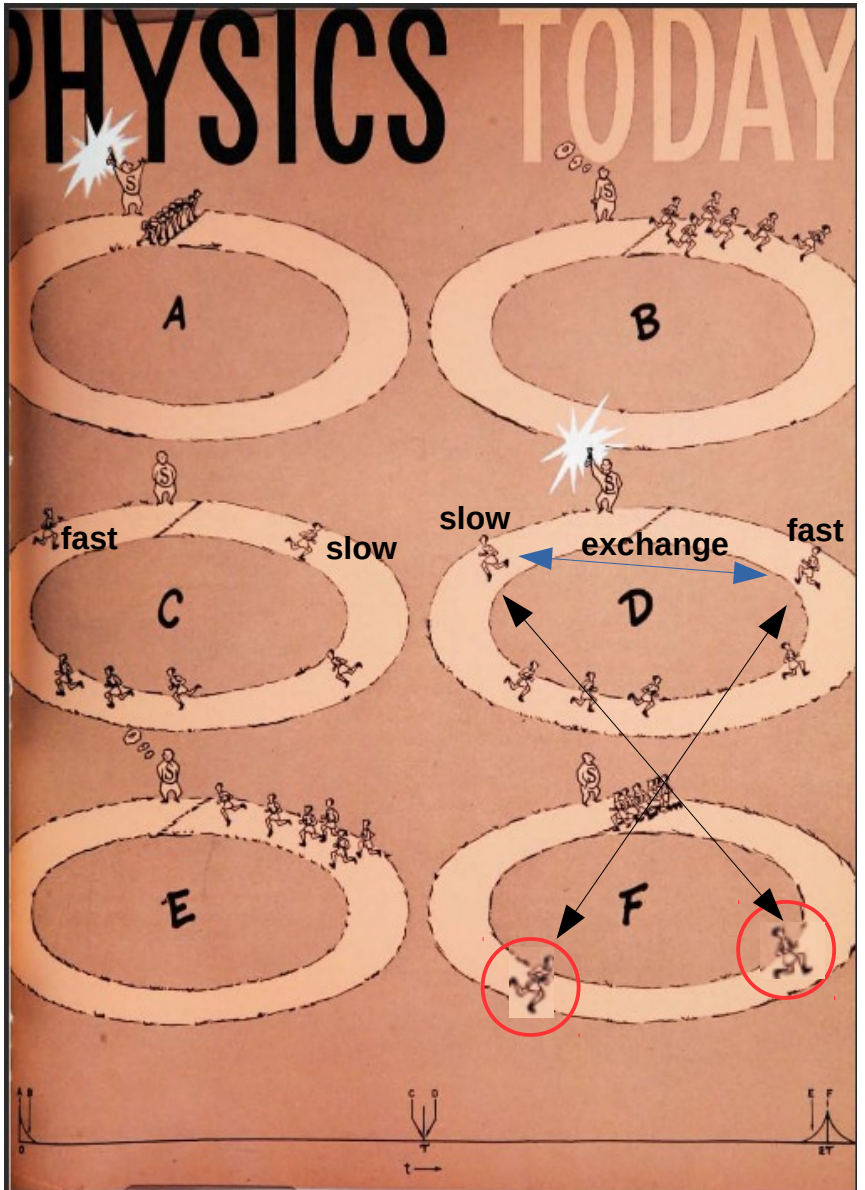

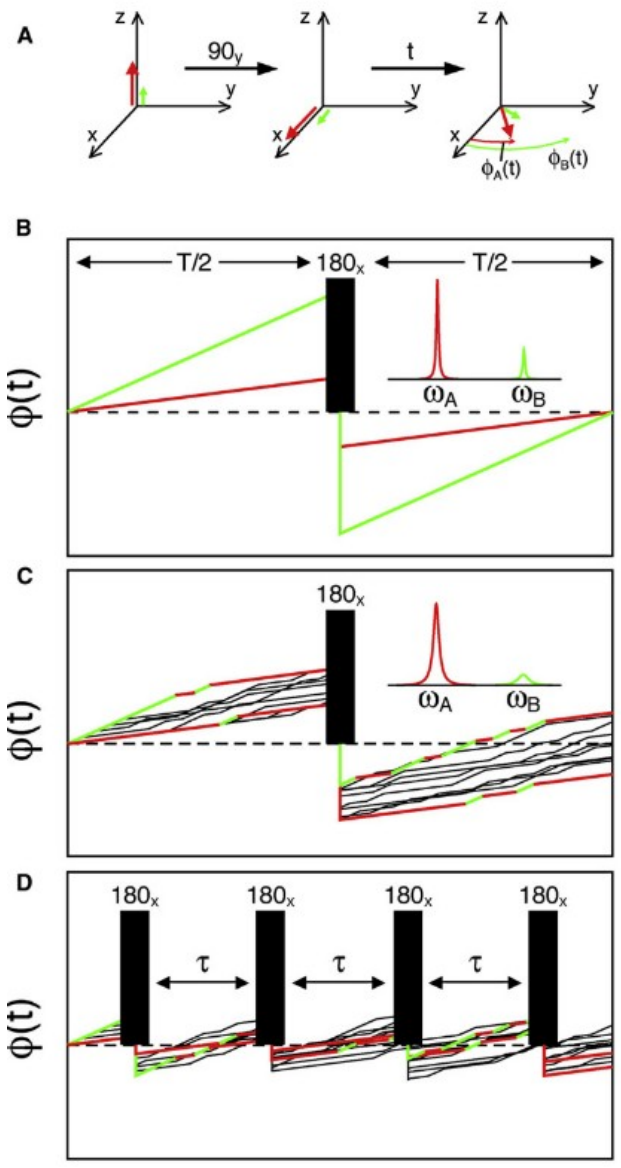

Erik Walinda, Daichi Morimoto, Kenji Sugase Methods Volume 148, 15 September 2018, Pages 28-38

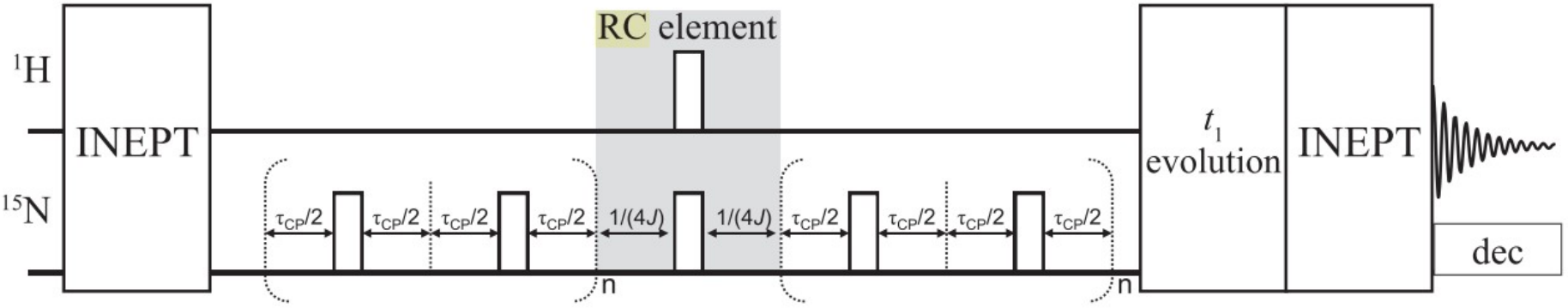

Fig. 5. R_2 relaxation dispersion pulse sequence. A simplified version of the relaxation-compensated ^{15}N CPMG relaxation dispersion experiment [20] is shown with the INEPT, ^{15}N chemical shift evolution, and reverse INEPT steps abbreviated. Open rectangles refer to 180° pulses. dec, decoupling sequence; RC, relaxation compensation.

Constant time CPMG

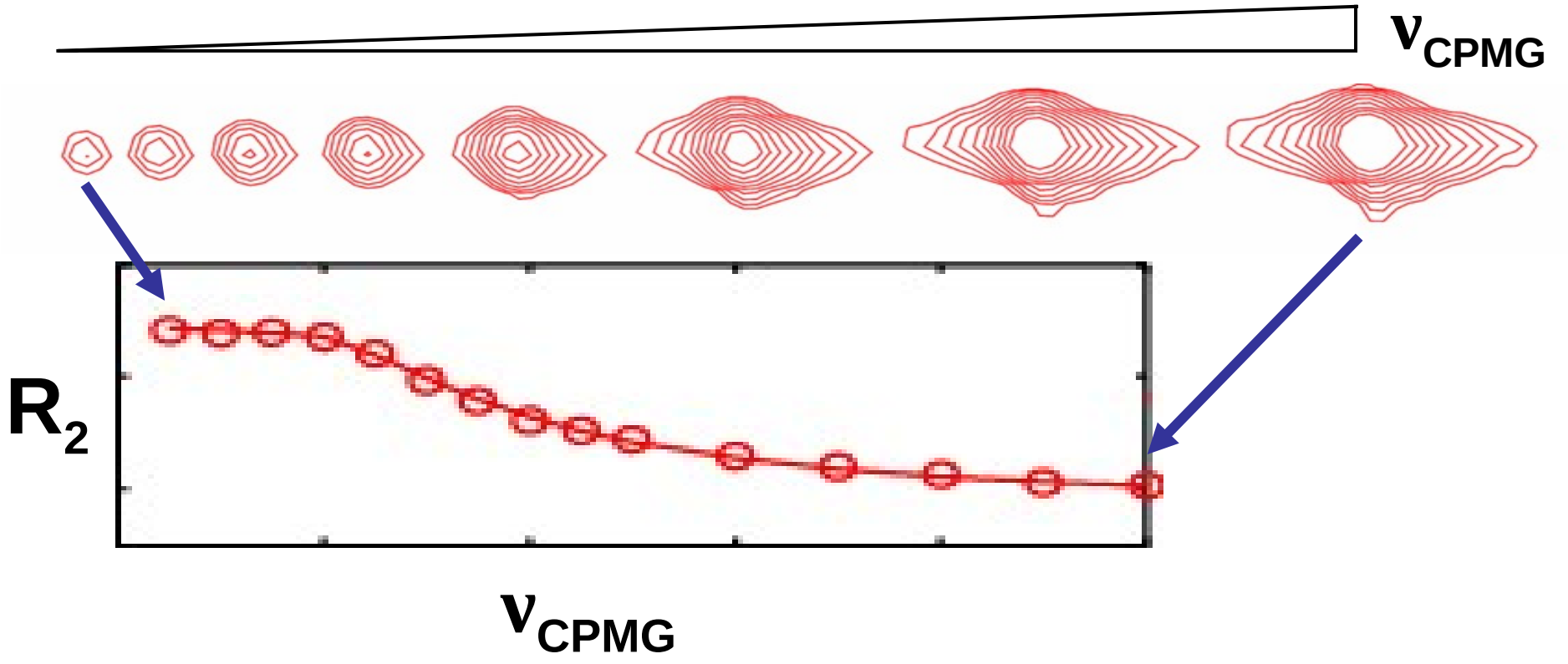

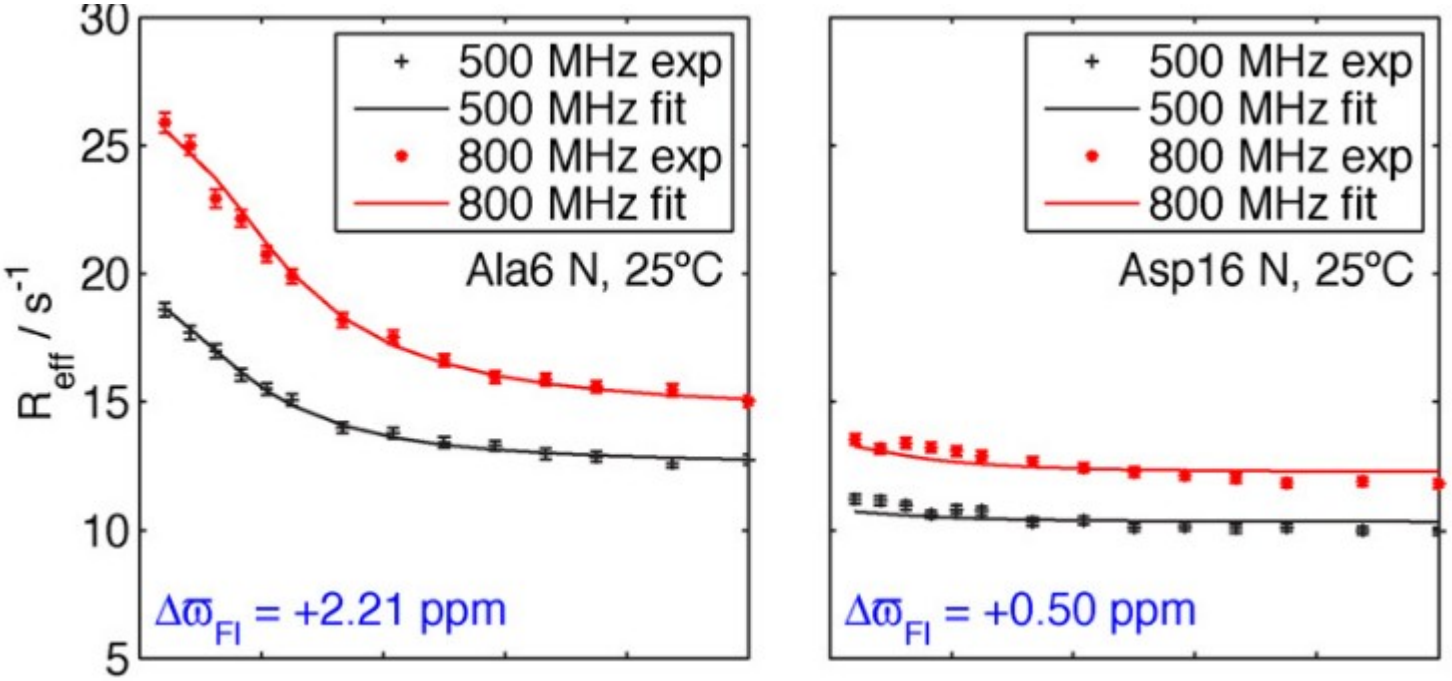
30
25
20
15
10
5
R_{eff} / s^{-1}
500 MHz exp
500 MHz fit
800 MHz exp
800 MHz fit
Ala6 N, 25°C
$\Delta\varpi_{FI}$ = +2.21 ppm
500 MHz exp
500 MHz fit
800 MHz exp
800 MHz fit
Asp16 N, 25°C
$\Delta\varpi_{FI}$ = +0.50 ppm

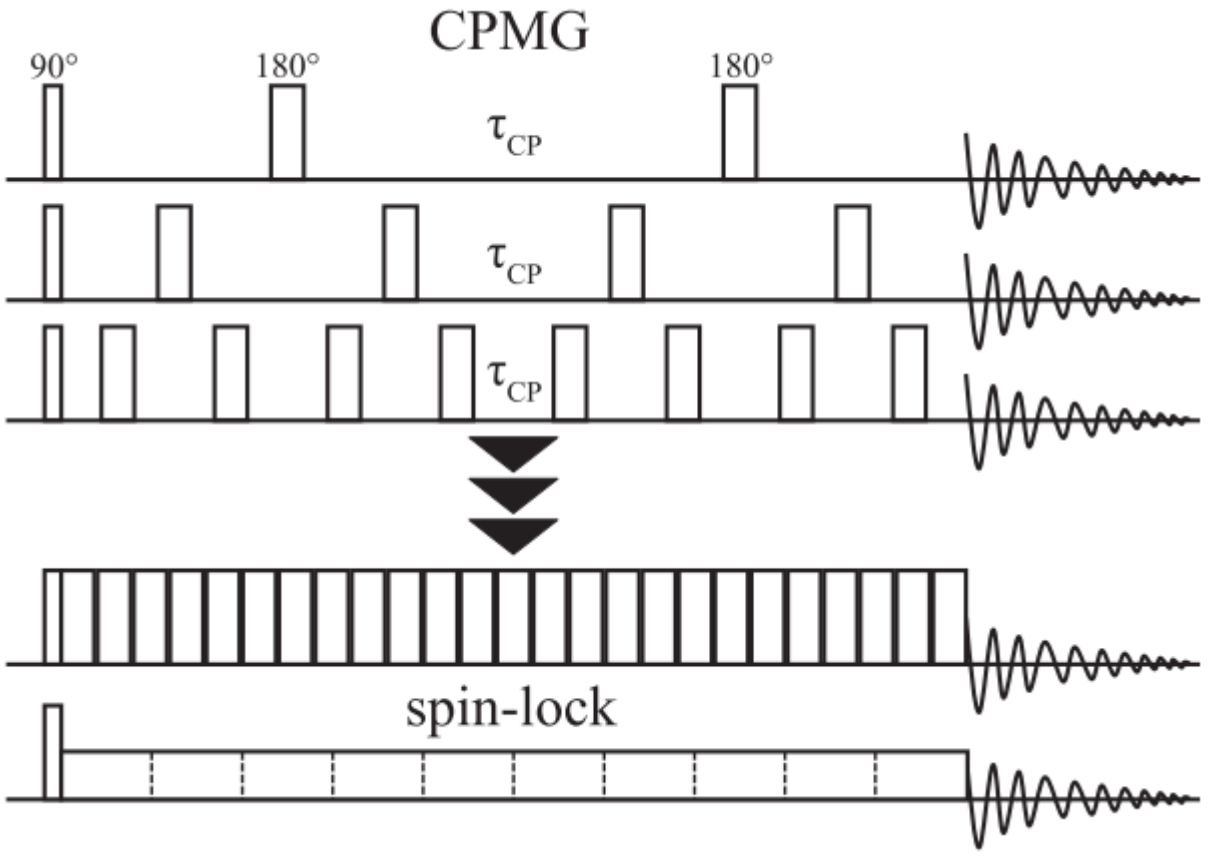
CPMG
90°
180°
180°
τCP
τCP
τCP
spin-lock

Effective field for T1rho

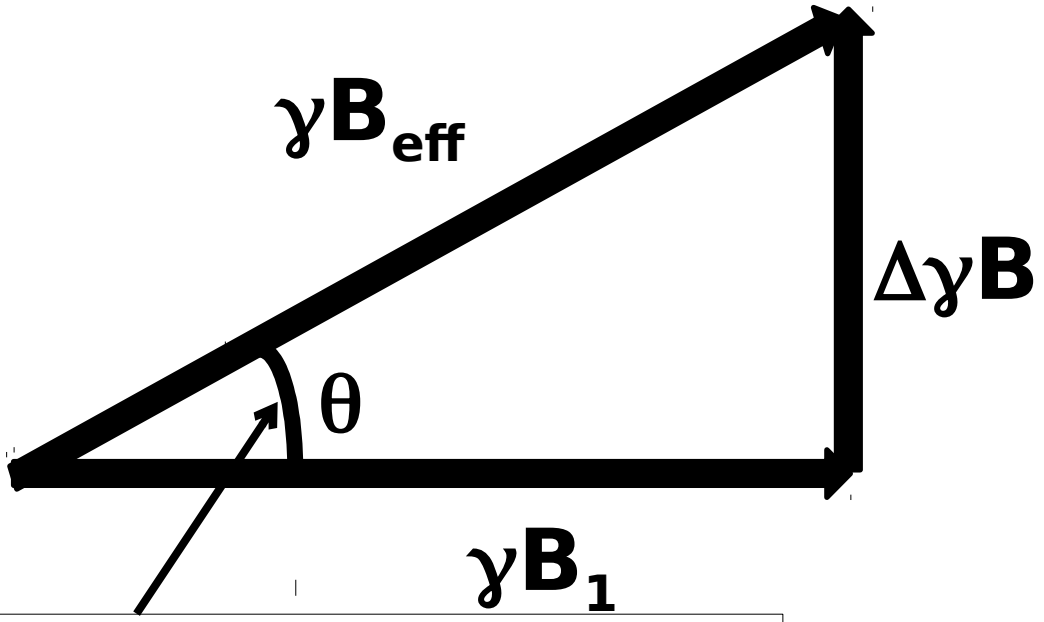

$$\theta = \tan^{-1}(\Delta\gamma B/\gamma B_1)$$

$$\gamma B_{eff} = \Delta\gamma B/\sin(\theta)$$

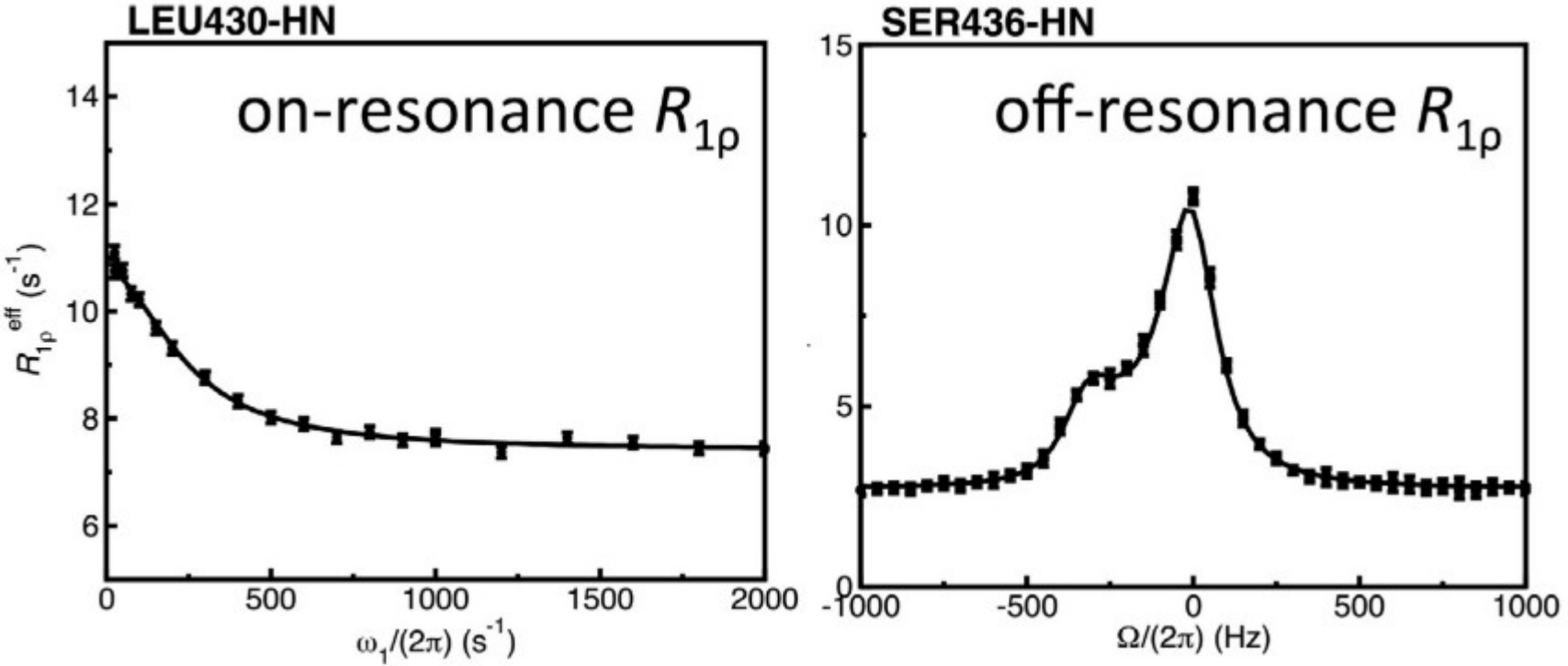

Fig. 3. Examples of R1ρ dispersion profiles. The two variants of the experiment are shown. In the left panel, the spin-lock power is varied; in the right panel, the power is kept constant while the spin-lock offset is varied. Figure reproduced with permission from Ref. [32].

Can measure faster rates with $T1_{rho}$ (1-6 kHz) – (CPMG 1-2kHz)

1D or 2D

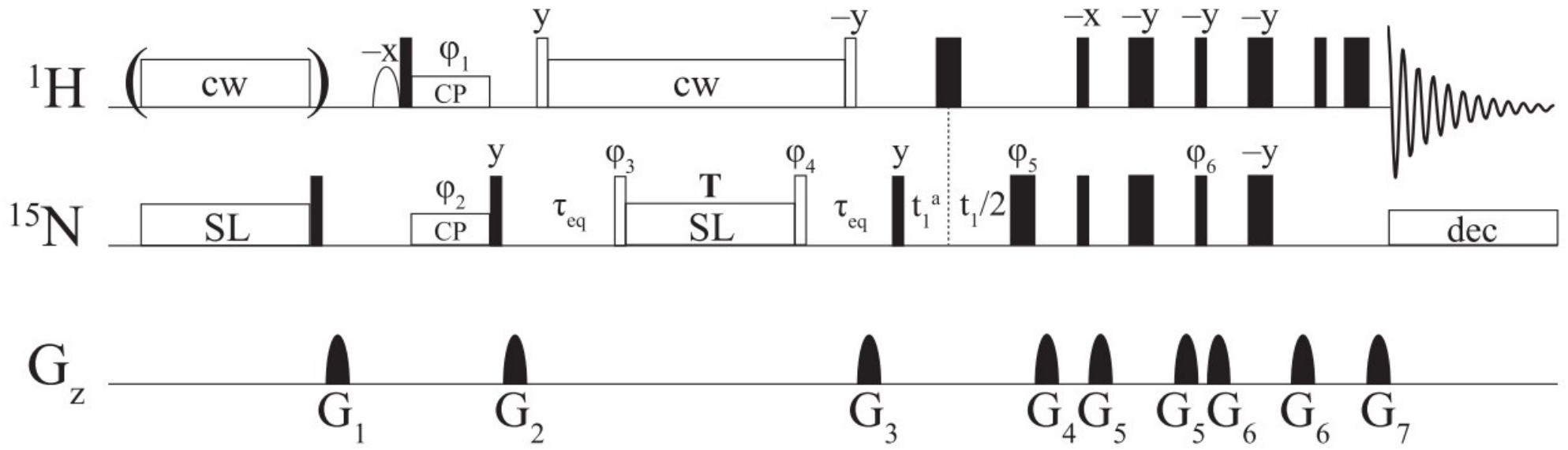

Fig. 6. $R_{1\rho}$ relaxation dispersion pulse sequence. The pulse diagram shows a selective sequence for probing one resonance at a time (reproduced with permission from Ref. [31]). Open rectangles denote pulses with varying tip angles [23]; filled rectangles refer to non-selective pulses. CP, cross-polarization; cw, continuous-wave; SL, spin-lock; dec, decoupling sequence. Pulses are applied with either *x*- or the indicated phase.

On- and off-resonance R1ρ relaxation profiles are recorded one residue at a time using a series of one-dimensional experiments in concert with selective Hartmann-Hahn polarization transfers.

Korzhnev, Dmitry M., Vladislav Yu Orekhov, and Lewis E. Kay. 2005. “Off-Resonance R1ρ NMR Studies of Exchange Dynamics in Proteins with Low Spin-Lock Fields: An Application to a Fyn SH3 Domain.” Journal of the American Chemical Society 127 (2): 713–21. doi:10.1021/ja0446855.

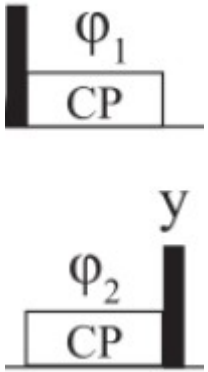

Hartmann-Hahn cross polarization in liquids

$$\xrightarrow{\pi J t I \cdot S} \equiv \xrightarrow{\pi J t \widehat{I_x S_x}} \xrightarrow{\pi J t \widehat{I_y S_y}} \xrightarrow{\pi J t \widehat{I_z S_z}} \text{in any order since they all commute}$$

$$I_z \xrightarrow{\frac{\pi}{2} I_x} -I_y \xrightarrow{\pi J t \widehat{I_y S_y}} -I_y$$

$$\xrightarrow{\pi J t \widehat{I_x S_x}} -I_y \cos(\pi J t) - I_z S_x \sin(\pi J t)$$

$$\xrightarrow{\pi J t \widehat{I_z S_z}} [-I_y \cos(\pi J t) + I_x S_z \sin(\pi J t)]\cos(\pi J t)$$
$$[-I_z S_x \cos(\pi J t) - S_y \sin(\pi J t)]\sin(\pi J t)$$

For $t = 1/2J$: $\cos(\pi J t) = 0$ $\sin(\pi J t) = 1$

$$= -S_y$$

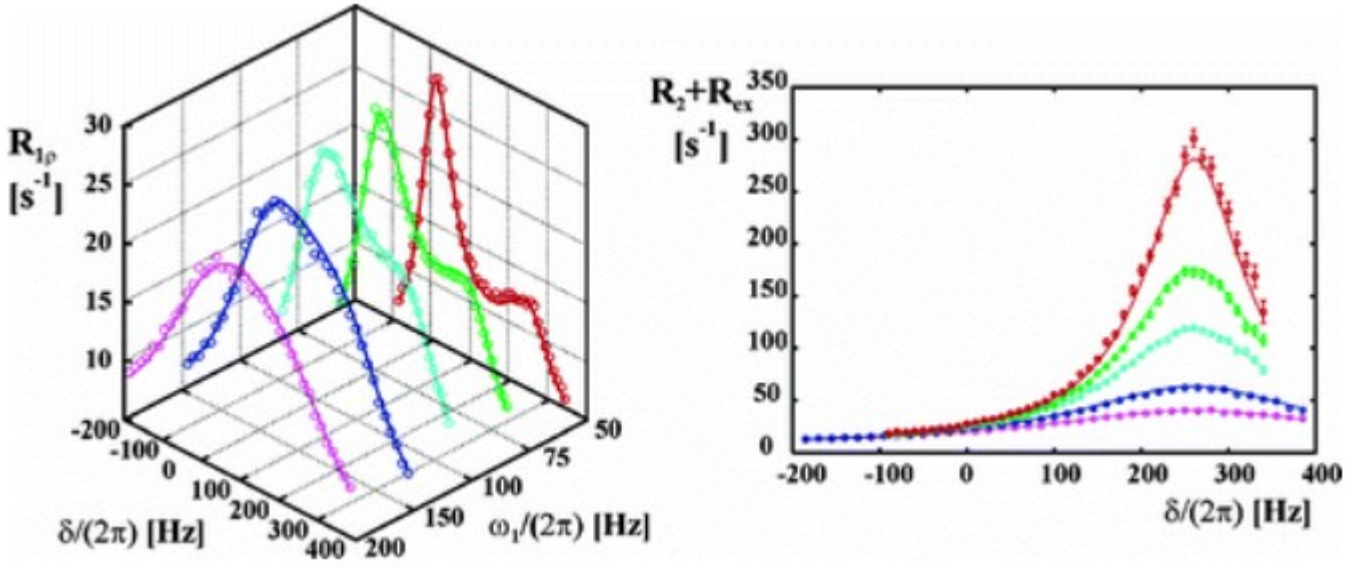

An 15N NMR R1ρ relaxation experiment is presented for the measurement of millisecond time scale exchange processes in proteins. On- and off-resonance R1ρ relaxation profiles are recorded one residue at a time using a series of one-dimensional experiments in concert with selective Hartmann−Hahn polarization transfers. The experiment can be performed using low spin-lock field strengths (values as low as 25 Hz have been tested), with excellent alignment of magnetization along the effective field achieved. Additionally, suppression of the effects of cross-correlated relaxation between dipolar and chemical shift anisotropy interactions and 1H−15N scalar coupled evolution is straightforward to implement, independent of the strength of the 15N spin-locking field. The methodology is applied to study the folding of a G48M mutant of the Fyn SH3 domain that has been characterized previously by CPMG dispersion experiments. It is demonstrated through experiment that off-resonance R1ρ data measured at a single magnetic field and one or more spin-lock field strengths, with amplitudes on the order of the rate of exchange, allow a complete characterization of a two-site exchange process. This is possible even in the case of slow exchange on the NMR time scale, where complementary approaches involving CPMG-based experiments fail. Advantages of this methodology in relation to other approaches are described.

Other References

Chemical exchange in biomacromolecules: Past, present, and future Arthur G. Palmer III, J Magn Reson. 2014 April ; 241: 3–17. doi:10.1016/j.jmr.2014.01.008